

Best Available Copy

J Oral Maxillofac Surg
50:140-151, 1992

Accelerated Endochondral Osteoinduction in the Absence of Bone Matrix Particles in a Rat Model System

ROGER SPAMPATA, DMD,* JOHN R. WERTHER, DMD, MD,†
AND PETER V. HAUSCHKA, PhD‡

Ethanol-precipitated proteins obtained from demineralized rat bone powder (DBP) by 4M guanidine-HCl extraction have been shown to reproducibly induce ectopic endochondral bone formation when subcutaneously implanted in rats in the absence of bone matrix particles. Histologic and biochemical analysis revealed a temporal sequence of chondrocyte differentiation, calcified cartilage formation, neovascularization, osteoblast differentiation, bone formation, osteoclastic bone remodeling, and hematopoietic marrow development that is complete by 21 days. In contrast to previous reports, these results clearly show an osteoinductive response independent of the presence of insoluble extracellular bone matrix. Compared with conventional DBP implants, the guanidine-extractable protein (GE) produces an accelerated and more robust osteoinductive response. Histologically, the initial chondrogenic response at days 6 to 9 is greatly amplified. Alkaline phosphatase specific activity peaks at day 9, several days earlier than for DBP, and is sixfold higher. Calcium accumulation in GE implants at day 12 is fivefold greater than with DBP, and all mineral is localized within the matrix of newly calcified cartilage and new bone. Osteoclasts are up to ninefold more abundant in the rapidly remodeling GE ossicle, making space for hematopoietic marrow. Delivery of GE coprecipitated with inert bone matrix particles was also more effective than DBP, although the response was somewhat attenuated compared with GE alone. Bony filling of 4-mm defects in rat mandibular rami was elicited by 10 mg of GE and followed an endochondral process with increased neovascularization compared with DBP and unimplanted controls. This guanidine-extractable protein fraction should prove useful for inducing quantities of chondrocytes and osteoclasts for in vitro study, and for analysis of osteoinductive requirements. Likewise, ethanol-precipitated osteoinductive proteins implanted alone or with carrier particles hold promise for use in reconstructive surgery.

More than a century has passed since Senn reported that the implantation of HCl-demineralized ox tibia into surgical defects could induce new bone formation.

* Chief Resident, Department of Oral and Maxillofacial Surgery, Sinai Hospital of Detroit, Detroit, MI.

† Assistant Professor, Department of Oral Surgery, Vanderbilt University School of Medicine, Nashville, TN.

‡ Associate Professor of Oral Biology and Pathophysiology, Harvard School of Dental Medicine, and Research Associate in Orthopaedic Surgery, Children's Hospital, Boston, MA.

Supported by the Phineas W. Sprague Memorial Foundation and NIH grants AR38349 and DE08519.

Address correspondence and reprint requests to Dr Hauschka: Department of Orthopedic Research, Enders-12, 300 Longwood Ave, Boston, MA 02115.

© 1992 American Association of Oral and Maxillofacial Surgeons
0278-2391/92/5002-0008\$3.00/0

Only within the last 25 years, however, has an understanding of the nature of this phenomenon developed, beginning with Urist's landmark demonstration of induced bone formation in rats in response to implanted demineralized, lyophilized bone.¹ The detailed study of osteoinduction was made possible through the subsequent development by Reddi and Huggins² of a demineralized bone powder (DBP) implant model that recapitulates the temporal sequence of endochondral ossification at an ectopic, subcutaneous site during a 3-week period.

In a conventional DBP implant, containing the natural mixture of osteoinductive and growth factor proteins, differentiation of chondrocytes is observed days 6 to 9. Calcification of the cartilage matrix is absorption by multinucleated chondroblast/osteoclast

and neovascularization are key processes that are initiated before the first appearance of osteoblasts and formation of bone by day 9 to 12. Osteogenesis and bone remodeling are prominent during days 12 to 21, and development of hematopoietic marrow begins about day 16, peaking at day 20 to 24.³

Sampath and Reddi⁴⁻⁶ developed a reconstitution assay with this model that allowed the isolation and purification of several different osteoinductive factors from the 4M guanidine-HCl extract of DBP. Cloning of these proteins has included bone morphogenetic proteins (BMPs),^{7,8} osteogenin,^{6,9} and osteogenic protein-1 (OP-1).^{10,11} All of these molecules are now recognized to be members of the transforming growth factor- β (TGF- β) superfamily of growth and differentiation factors.^{7,11}

The ability of recombinant osteogenic proteins, particularly OP-1 and BMP-2, to initiate the cascade of osteoinduction when presented in nanogram to microgram quantities on collagenous carrier matrix particles has been demonstrated.^{7,8,10} The recruitment and commitment of mesenchymal cells within the first 3 days appears to be important in the initial stage of osteoinduction.^{3,12} However, it is not clear if these cells then take over control of the process by themselves, or if they require the sequential input at critical times of paracrine factors from other cell types to complete the temporal cascade.^{12,13}

Translation of this well-studied animal osteoinduction model into practical procedures for human craniofacial and orthopedic surgery has been a longstanding goal.^{1,14,15} With the promise of developing pure recombinant osteoinductive proteins in large amounts, attention is focusing on implant formulations and delivery systems for these factors that will maximize and sustain the biological response.¹⁶⁻¹⁸ Osteointegration of the induced bone tissue with the margins of host bone also is critical.¹⁹

The osteoinductive response to implanted materials is strongly dependent on both the rate of release of OP-1/BMP-2/osteogenin factors and the surface characteristics and molecular environment into which wandering or chemotactically attracted mesenchymal cells are drawn. Reddi and coworkers have consistently maintained that geometry of the implanted matrix plays a crucial role in generating the osteoinductive response. They reported that osteoinduction occurred solely in response to implanted DBP of a specific particle size range (74 to 420 μ m).⁵ Likewise, when the osteoinductive activity (either in the form of the ≤ 50 kDa 4M guanidine-HCl-soluble fraction or the 12,000-fold purified osteogenin) was reconstituted with the inactive 4M guanidine-HCl-insoluble bone matrix particle residue (GR) prior to implantation, osteoinduction ensued only if the matrix particles were 74 to 420 μ m in size. Reconstitution of osteoinductive proteins with matrix particles of a size 44 to 74 μ m reportedly pro-

duced no response.^{3,5,20} Similarly, when the osteoinductive protein fraction was implanted alone, without matrix particles, there was a lack of osteoinduction.^{3,5,20} These findings have led to the conclusion that bone matrix particles of a limited size distribution are essential for 1) providing a substratum for mesenchymal cell anchorage, proliferation, and differentiation, and 2) presenting osteoinductive factors to invading mesenchymal cells.^{3-5,20}

Challenging such a hypothesis, work in our laboratory has shown that the ethanol precipitate of the 4M guanidine-HCl extract of rat DBP will reproducibly initiate osteoinduction when implanted subcutaneously in rats in the absence of bone matrix particles.^{21,22} Presented here are experiments that characterize and compare the osteoinductive responses to rat bone proteins implanted in the presence and absence of bone matrix particles.

Materials and Methods

Implant preparation. Bone powder was prepared from the long bones of mixed-age, mixed-sex Sprague-Dawley and Long-Evans strain inbred rats by a modification of previous methods.^{2,23} Bones were dissected and cleaned of adherent soft tissue on ice, ground in 10 changes of 4°C deionized water in a Waring blender and then with a Polytron (Brinkman), and sedimented at 1xg. Water-washed powder was defatted and dehydrated by suspending three times in 20 volumes of absolute ethanol, twice in anhydrous diethyl ether, and then air dried by suction on a Buchner funnel. Further grinding at -196°C in a Spex mill (Spex, Inc, Metuchen, NJ) yielded 80% to 90% of the original bone in the 74- to 250- μ m size range. To prepare DBP, sieved powder (50 g, 74 to 250 μ m) was washed with 900 mL 20 mM Tris-HCl, pH 7.6, for 20 min at 4°C, centrifuged at 1,000xg for 10 min, and resuspended in 750 mL 0.5 N HCl at 4°C for 1 hour. After centrifugation, the powder was further demineralized in 1,750 mL 0.5 N HCl at 23°C for 2 hours. The DBP was washed six times in 1,800 mL 4°C water for 10 minutes and recovered by centrifugation. After three ethanol washes and two diethyl ether washes (500 mL each, 10 minutes, 4°C), the DBP was air dried and stored at -20°C (yield, approximately 220 mg DBP/g bone powder). Nonosteoinductive bone powder residue (GR) was prepared by further extracting DBP with 4M guanidine-HCl, 50 mM tris, pH 7.6 (30 mL/g DBP, 16 hours, 4°C) as outlined by Sampath and Reddi,⁴ with the notable exception that proteinase inhibitors were not used. Dialysis against deionized water at 4°C (Spectrapor 3, 3.5 kDa cutoff; Spectrum Medical Ind, Los Angeles, CA) and lyophilization yielded the guanidine-extractable protein fraction (designated as GE) containing osteoinductive activity (yield, approximately 7 mg GE/100 mg DBP). The insoluble residue (GR; 74 to 250 μ m) was collected and washed six times with water, as

for DBP above, lyophilized, and stored at -20°C (yield, ≈ 620 mg GR/g DBP).

Implant formulation. Four general types of implants were studied as shown in Table 1: GE in amounts of 2 to 20 mg delivered alone (GE2, GE5, GE10, GE20) or in combination with 25 mg of GR carrier (RG2, RG5, RG10, RG20); DBP or GR (25 mg, 74 to 250 μm) were used as positive and negative controls, respectively. RG implants were prepared by a modified ethanol reconstitution protocol.⁴ For example, to prepare 20 individual implants designated RG20, 400 mg of GE was dissolved in 8 mL 4M guanidine-HCl, 50 mM tris, pH 7.4, making a clear solution. Next, this solution was pipetted into a 50-mL polypropylene centrifuge tube containing exactly 500 mg of dry GR particles. The tube was capped and rotated for 12 hours at 4°C . Ice-cold absolute ethanol (32 mL) was then added to precipitate the GE proteins. The resulting precipitate was centrifuged after 2 hours on ice, washed five times in 40 mL cold 85% ethanol, and lyophilized. The large dry pellet was subdivided into 20 45-mg implants (20 mg GE + 25 mg GR) by weighing. To prepare 20 implants of GE20, all steps were identical, except that 400 mg of GE was ethanol-precipitated in the absence of GR; after washing with 85% ethanol and lyophilizing, the pellet was subdivided into 20-mg implants by weighing. Other GE and RG implants were prepared accordingly. To test the importance of ethanol precipitation, one batch of ethanol-precipitated and dried GE was redissolved in 4M guanidine-HCl, 50 mM tris, pH 7.4, dialyzed (3.5 kDa cutoff) against water 48 hours at 4°C , and lyophilized. The 20-mg dry-weight implants of this material were designated GED20.

Surgical placement of implants. Individually weighed implants were moistened with sterile water, packed into the hubless end of a 0.5-mL plastic syringe, and sealed with Parafilm (Fisher Scientific, Pittsburgh, PA) until the time of implantation. As described by Reddi and Huggins,² male 28- to 35-day-old Long-Evans strain rats (Charles River Laboratories) were individually anesthetized by brief exposure to ether in a sealed chamber. Bilateral 1-cm incisions just below the costal margins were dissected bluntly toward the thoracic region, creating 3-cm blind subcutaneous pockets

into which the implants were expressed at the pectoral level by syringe. The incisions were closed with 9-0 stainless steel wound clips and the animals returned to their labeled cages. A total of 716 implants placed in 358 rats in six experiments were distributed as follows: 148 DBP, 148 GR, 8 GE2, 28 GE5, 62 GE10, 28 GE20, 68 GED20, 36 RG2, 28 RG5, 62 RG10, and 96 RG20. No animals died during the implantation procedure and the survival rate until killing was $>99\%$.

Surgical filling of mandibular defects. Circular cortical defects of 4 mm diameter critical size were prepared bilaterally under general anesthesia (1% amine/xylazine) in the mandibular rami of 500-g Long-Evans strain rats.²⁴ Defects ($n = 5$ per group per time point) were filled with 10 mg GE or 25 mg DBP (positive control) or irrigated with sterile saline (negative control), and closed surgically. Animals were killed after 14 and 21 days, and hemimandibles were processed for histology.

Implant recovery and analysis. At intervals from day 2 to 42 after implantation, rats were anesthetized with ether, and blood samples were taken. After exsanguination by ether inhalation, the implants were surgically dissected, cleaned of soft tissue adherent to the fibrous capsule, promptly weighed, sampled for histology, and frozen at -80°C .

Histology and histomorphometry. Histological specimens cut from selected implants were fixed in 10% formalin-0.1M cacodylate, pH 7.2, for 1 week and embedded in JB-4 medium (Polysciences, Warrington, PA). Undecalcified 3- μm sections were stained with von Kossa's stain for mineral (3% AgNO_3) and counterstained with 1% toluidine blue. Tissue blocks and sections for tartrate-resistant acid phosphatase (TRAP) staining were stored at 4°C . A modification of the method of Troyer et al²⁵ involved incubation with freshly prepared 0.1% naphthol AS-MX (free acid, Sigma, St Louis, MO), 0.2% Fast Red TR (Sigma), 0.1M tris-0.1 M tartrate, pH 5.0 for 30 min at 37°C . Slides were rinsed and counterstained with toluidine blue.

Histomorphometry was accomplished with a ZIAD semiautomated image analyzer (Zeiss, Thornwood, NJ). Stained slides to be examined were blindly numbered and examined in random order. Decoding was done only after all measurements on all slides were completed. Six random fields (200 \times) from each of at least two specimens taken from each implant group at each time point were examined. Parameters evaluated were osteoclasts/ mm^2 bone section, cartilage as percentage of field, and bone as percentage of field.

Chemistry. Bone formation was quantitated by alkaline phosphatase activity and calcium content. Alkaline phosphatase activity was determined by the method of Reddi and Huggins.² Weighed implants samples were subjected to three freeze/thaw cycles, homogenized on ice in 2 mL of 0.15 M NaCl , 0.1 M NaHCO_3 , pH 7.4. After transfer to a microtiter

Table 1. Experimental Design

Implant Group	Treatment*	Dosage (mg)
GE	1	GE alone: 2, 5, 10, 20
GED20	2	GE alone: 20
RG	3	GR: 25 plus GE: 2, 5, 10, 20
GR	4	GR alone: 25 (negative control)
DBP	4	DBP alone: 25 (positive control)

* Treatment: 1, ethanol precipitated; 2, ethanol precipitated, redissolved in 4M guanidine-HCl, water dialyzed, lyophilized; 3, ethanol precipitated from 4M guanidine-HCl solution in presence of GR; 4, water washed, lyophilized; see Methods.

ctoral
1-mm
ed to
ed in
llows:
E20,
G20
ture

ar bi-
were
(ket-
ing
time
(pos-
tive
dai-
ssed

om-
zed
cu-
rgi-
the
is-
sic

10%
and
on
with
un-
ind
VP)
the
ith
id
0.2
10
15
20
25
30
35
40

and centrifugation at 11,000 \times g for 2 min, supernatants were stored at -80°C until assay. Samples (1 to 100 μ L) were assayed in 0.1 M sodium barbital, pH 9.4, containing 5 μ mol p-nitrophenylphosphate substrate (Sigma) in a total volume of 1 mL; after 1 hour at 37°C the reaction was stopped with 1 mL 1M NaOH and absorbance was measured at 400 nm with p-nitrophenol as a standard. Background from hemoglobin absorbance (410 nm maximum) in highly vascularized implants was corrected by subtraction of enzyme blanks (no substrate added). Specific activity was calculated as nmol p-nitrophenol liberated/min/mg protein. Protein was determined by the dye-binding method of Bradford.²⁶ Calcium content of 550°C ashed samples dissolved in 5% lanthanum oxide, 3 N HCl was measured by atomic absorption spectrophotometry.

Hematology. Hematocrits were determined at sacrifice by filling 7.5-mm heparinized capillary tubes (Chase, Glen Falls, NY) with blood, spinning 5 minutes on a microcapillary centrifuge, and reading on a microcapillary reader (Damon, Needham, MA). Total white blood cell counts were determined with a Unopette microcollection system (Thomas Scientific, Boston, MA) and a hemocytometer slide chamber (Neubauer; Thomas Scientific).

Statistics. One-way analysis of variance (ANOVA) was used to compare means of groups within each experiment. The *t* test was used to analyze the significance of differences between mean values of paired data. *P* values less than .05 were considered significant.

Results

Analysis of recovered subcutaneous implants showed that the DBP group produced the expected osteoinductive response, while the GR group provided a suitable nonosteoinductive control (Figs 1-3, Table 2). The

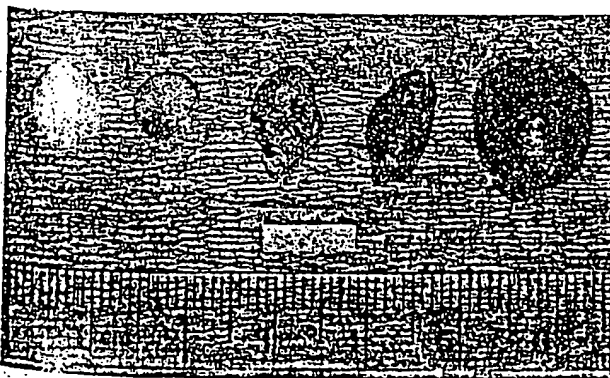


FIGURE 1. Gross appearance of implants recovered from rats after 21 days. From left: GR (negative control), DBP (positive control), GE10 (10 mg GE protein), GE20 (20 mg GE protein), RG20 (20 mg GE protein on 25 mg GR carrier). Note the increased size of the RG20 implant: The dark pigmentation reflects the extensive neovascularization and hematopoiesis occurring in the GE and RG samples. Bar = 10 mm.

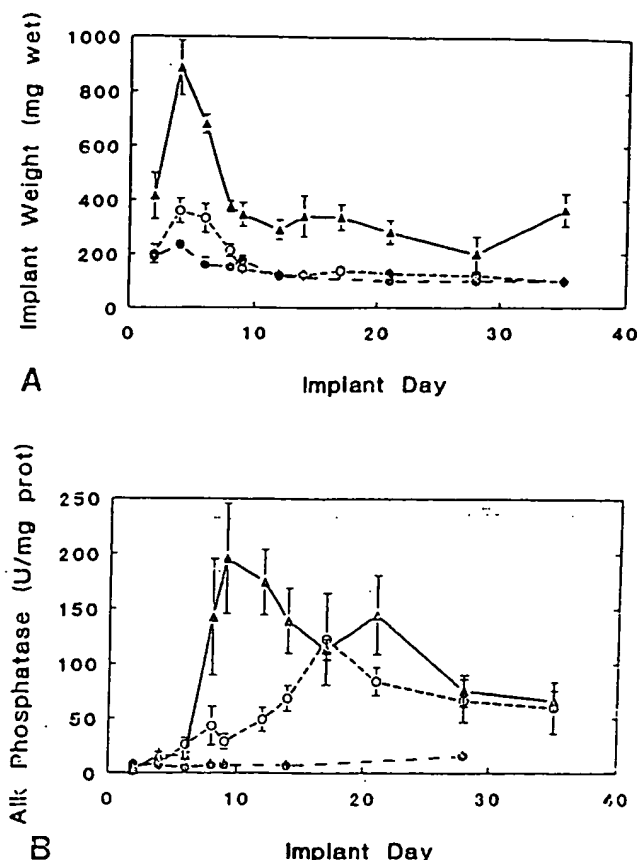


FIGURE 2. *A*, Weights of subcutaneous implants procured on different days. Implant groups: GR (solid circles), DBP (open circles), and RG20 (solid triangles). Data represent mean wet weights \pm SEM ($n = 10$). Weights of RG20 were significantly greater than DBP and zGR at days 2 to 21 and day 35 ($P \leq .05$); DBP weight was significantly greater than that of GR at days 4 to 6 ($P \leq .01$). *B*, Alkaline phosphatase-specific activities of procured implants. Symbols are as in 2A. Data represent mean units (nmol p-nitrophenol formed/min/mg soluble protein) \pm SEM ($n = 10$). Activities of RG20 were significantly greater than DBP at days 8 to 14 ($P \leq .05$); RG20 and DBP were significantly greater than GR at days 6 to 35 ($P \leq .01$).

gross appearance of the implants changed over time as expected. At early points (days 3 to 9) all implants were soft and white in color. The connective tissue capsules surrounding the implants were difficult to remove without breaking up the specimens. The GR implants retained this appearance through day 42 and developed a nonmineralized capsule. However, the DBP, GE, and RG implants began to develop a firmer consistency by day 9. Concomitant with this change was an intensifying pink color on the implant surface. Through day 21 the changes progressed to the point of deep red color and hard, solid form, particularly for GE20 and RG20 (Fig 1).

Mean weights of implants peaked at days 4 to 8, with the greatest size found for RG20 (Fig 2A). Its mean weight of 887 ± 145 mg at day 4 was considerably greater than its day 0 preimplantation weight of approximately 150 mg wet (45 mg dry), and significantly greater than day 4 DBP (2.5-fold) and GR (fourfold).

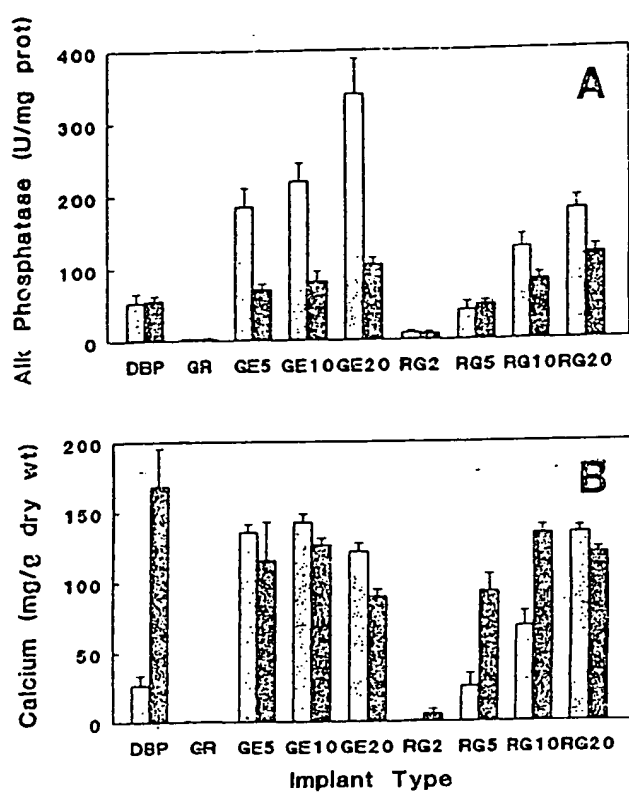


FIGURE 3. Dependence of osteoinductive response on implant formulation. Implant groups included DBP (25 mg, positive control), GR (25 mg, negative control), three doses of GE (5 mg, GE5; 10 mg, GE10; 20 mg, GE20), and four doses of GE coprecipitated with 25 mg of GR (2 mg, RG2; 5 mg, RG5; 10 mg, RG10; 20 mg, RG20). Implants were procured from host rats at day 12 (shaded bars) and day 21 (black bars); data represent means \pm SEM ($n = 10$). A, Alkaline phosphatase specific activities. Activities of all groups except RG2 are significantly greater than GR at days 12 and 21 ($P \leq .01$); groups with activities exceeding DBP include GE5, GE10, GE20, RG10, and RG20 at day 12 ($P \leq .01$), and GE10, GE20, and RG20 at day 21 ($P \leq .01$). Both the GE and RG groups show significant dose-dependence with increasing amounts of implanted GE protein. The sixfold increase of activity in day 12 GE20 versus DBP is evidence of the acceleration and augmentation of the osteoinductive response. The RG group also shows these effects, but adsorption of GE to the GR particles modulates the response. B, Calcium contents. Mineralization of all implant groups except RG2 is significantly greater than GR at days 12 and 21 ($P \leq .01$); groups with calcium levels exceeding those of DBP include GE5, GE10, GE20, RG10, and RG20 at day 12 ($P \leq .01$), but differences have been lost by day 21 ($P \geq .1$). However, histology of DBP (Fig 6B) shows that much of the initial apparent calcium uptake involves remineralization of implanted DBP particles, in contrast to the true bone formation occurring in GE and RG samples. The approximately fivefold increase of GE and RG mineralization at day 12 compared with DBP is additional evidence for the acceleration and enhancement of osteoinduction by GE and RG implants.

($P \leq .01$). GE20 implants were intermediate in weight between RG20 and DBP (data not shown). The early peak in RG20 implant weight was correlated with the initial cellular reaction to this material, which causes transient formation of a cystlike structure containing serum-colored fluid. This also occurs with GE and DBP

of inflammation in the implants: 1) cathepsin B levels (data not shown) peaked at days 4 to 6 with equivalent specific activities in RG, GE, DBP, and GR specimens; 2) host animal white blood cell counts were not elevated. The mean weight of RG20 implants is maintained at approximately 300 mg from days 12 to 35, which is 2.5-fold more than DBP (approximately 121 mg) (Fig 2A). GE20 implants obtained at day 12 (approximately 198 mg) and day 21 (approximately 129 mg) show intermediate weights ($P \leq .05$).

ALKALINE PHOSPHATASE ACTIVITY AND CALCIUM CONTENT

The dependence of osteoinductive response on implant formulation was studied in a variety of implant groups including DBP (25 mg, positive control), GR (25 mg, negative control), three doses of GE (5 mg, GE5; 10 mg, GE10; 20 mg, GE20), one dose of dialyzed GE (GED 20 mg), and four doses of GE coprecipitated with 25 mg of GR (2 mg, RG2; 5 mg, RG5; 10 mg, RG10; 20 mg, RG20). Implants were obtained from host rats at days 12 and 21 in one large experiment (Fig 3), and at days 2 to 42 in five other experiments.

As shown in Fig 3A and Table 2, alkaline phosphatase specific activity reached its highest value for GE20 at day 12, some sixfold greater than the DBP positive control, and about 120-fold greater than the GR negative control. Activity of all groups except RG2 is significantly greater than GR at days 12 and 21 ($P \leq .01$). Activities exceeding that of DBP include GE5, GE10, GE20, RG10, and RG20 at day 12 ($P \leq .01$), and GE10, GE20, and RG20 at day 21 ($P \leq .01$).

Calcium analysis showed that mineralization of all implant groups except RG2 is significantly greater than GR at days 12 and 21 ($P \leq .01$). Calcium levels exceeding that of DBP include GE5, GE10, GE20, RG10,

Table 2. Comparative Osteoinductive Activity in Day 12 Implants

Implant Group	Alkaline Phosphatase (nmol/min/mg protein)	Calcium Content (mg/g dry wt)	Wet Weight (mg)
GE20	339.6 \pm 48.4*†	121.9 \pm 5.9*§	198.2 \pm 27.1
GED20	6.6 \pm 4.6‡	N.D.	19.1 \pm 3.0
RG20	178.3 \pm 17.4*§	135.3 \pm 4.3*§	404.2 \pm 42.1
GR	2.8 \pm 1.1	0.9 \pm 0.1	119.1 \pm 9.1
DBP	53.2 \pm 12.4*	26.8 \pm 7.2*	123.5 \pm 9.1

Means \pm SEM; $n = 10$ for all groups except GED20 ($n = 6$).

Abbreviation: ND, not done.

* Significantly different from GR ($P \leq .01$).

† Significantly different from DBP and RG20 ($P \leq .01$).

‡ Significantly different from GE20 ($P \leq .001$).

§ Significantly different from DBP ($P \leq .01$).

and RG20 at day 12 ($P \leq .01$), and the 9% to 13% content of calcium in day 21 GE and RG ossicles compares favorably with the levels of 18% to 24% in compact cortical bone. Differences between GE, RG, and DBP have been lost by day 21 ($P \geq .1$) (Fig 3B). However, histology of DBP (Fig 6B) shows that a significant fraction of the calcium uptake involves remineralization of implanted DBP particles, in contrast to the true bone formation occurring in GE and RG samples.

Acceleration of the osteoinductive cascade by GE and RG implants is demonstrated by the earlier expression of bone formation markers compared with DBP (Table 2, Figs 2B, 3). In another experiment, GE10 demonstrated 1.8-fold greater alkaline phosphatase activity ($P \leq .015$) and 4.3-fold greater calcium content ($P \leq .01$) than DBP at days 6 and 12, respectively. For the RG implants, RG10 reached a level of alkaline phosphatase activity 3.2-fold greater than that for DBP at day 9 ($P \leq .03$). Calcium content for RG10 was approximately fourfold greater than that for DBP at days 12 to 15 ($P \leq .04$). RG20 demonstrated maximal levels of alkaline phosphatase activity at day 8. At day 9, alkaline phosphatase activity of RG20 was 6.8-fold greater than that of DBP ($P \leq .02$), remaining at least three times greater than DBP through day 14 ($P \leq .05$) (Fig 2B). Peak calcium content of RG20 was reached at day 12, and the day 17 calcium content of RG20 was 2.4-fold that of DBP ($P \leq .03$).

Amplification of the osteoinductive response by GE and RG was shown by the achievement of greater maxima for bone formation markers than DBP. The sixfold increase of alkaline phosphatase activity in day 12 GE20 versus DBP is evidence of the acceleration and augmentation of the osteoinductive response. The RG group also showed these effects, but adsorption of GE to the GR particles modulated the response. In a dose-dependent manner, RG alkaline phosphatase was elevated over DBP at days 12 and 21, and calcium was elevated at day 12 (Fig 3, Table 2).

GED20 implants produced by dialysis rather than ethanol precipitation exhibited low alkaline phosphatase activity that did not differ at any time from that of the negative control GR (Table 2).

DBP and GR control implants. DBP produced an osteoinductive response as expected, showing greater alkaline phosphatase activity and calcium content than GR by day 6 and day 9, respectively. Alkaline phosphatase specific activity increased about 20-fold in the osteoinductive DBP implants at days 12 and 21 compared with the inactive GR controls. Calcium content of DBP specimens was elevated 29-fold at day 12 and 162-fold at day 21 compared with GR (Table 2 and Fig 3). Alkaline phosphatase activity and calcium content of GR implants did not increase beyond baseline. The temporal sequence of osteoinduction with DBP implants has been very reproducible in these and other experiments in our laboratory,^{21,22,27} and exactly par-

allels within ± 1 day the timing reported by Reddi and colleagues.²³

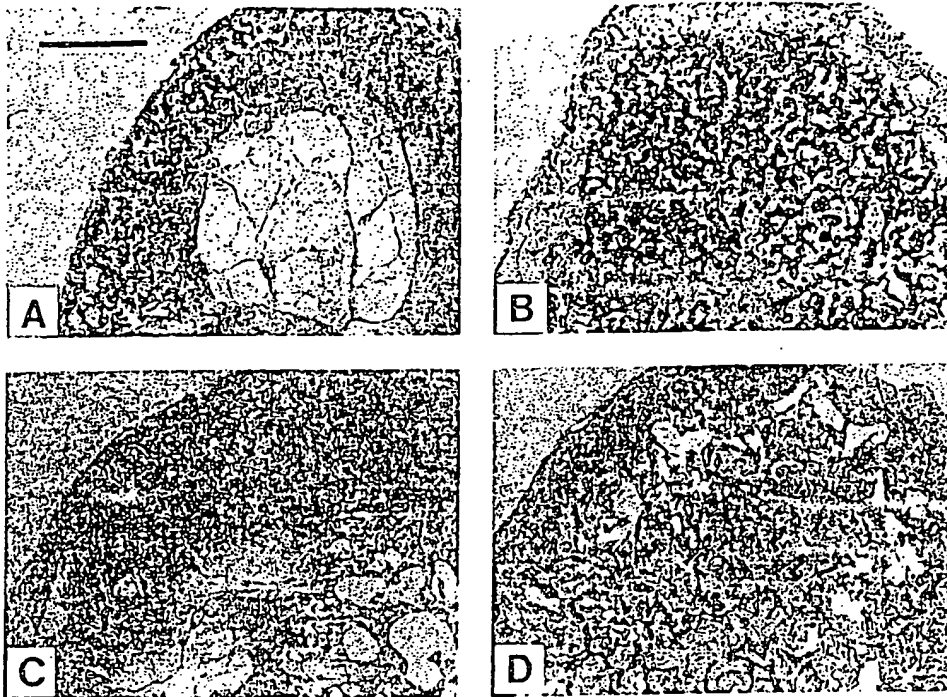
HISTOLOGY

A portion cut from the center of each implant was examined by light microscopy for evidence of osteoinduction at the various times of implantation. Endochondral bone formation was seen in response to implanted GE5, GE10, GE20, RG5, RG10, RG20, and DBP. There was a weak response to RG2, and GE2 was difficult to recover after implantation. No endochondral bone formation was seen in response to implanted GED20 or GR.

GE implants. At day 6, GE5, GE10, and GE20 implants were encapsulated with fibrous tissue. Invading mesenchymal cells with occasional leukocytes were evident surrounding aggregates of "fibrinoid" material (representing the implanted protein). Adjacent to and within this protein, large numbers of rounded chondroblasts/cytes had secreted metachromatic matrix around themselves. Chondrocytes were visible within the lacunae of mature cartilage. By day 9, GE implants contained extensive areas of new cartilage. Foci of mineralizing cartilage were evident along with areas of cells staining positively for alkaline phosphatase. At day 12 (Figs 4A, 5) areas of cartilage, mineralized cartilage, and vascularized cancellous bone were present (compare with day 12 DBP, Fig 6A). Alkaline phosphatase-positive cells and multinucleated TRAP-positive giant cells were abundant on mineralized surfaces, suggesting active osteoblasts and osteoclasts, respectively. Transmission electron microscopy of a day-12 GE10 implant showed the presence on bone and calcified cartilage of large multinucleated cells with abundant mitochondria and rough endoplasmic reticulum. At the junction of such cells and the mineralized surface there was a cytoplasmic clear zone, free of organelles, and a ruffled border characteristic of osteoclasts. On day 21, large venous sinusoids and marrow elements were clearly evident within the trabeculae of the heavily remodeled ossicle (Fig 4C, 7). Examination of GE implants over days 15 to 42 showed remodeling bone containing large marrow spaces and active, TRAP-positive osteoclasts (Figs 4C, 7, 8).

GED20 implants. In contrast to implants of GE10, GE20, RG10, RG20, DBP, and GR, which had a 90% to 96% recovery rate from the animals, implants of GED20 had only a 54% recovery rate. On days 2 to 4, GED20 implants appeared as yellow gelatinous masses, and by day 9 were small and difficult to locate under the skin. There was no histological evidence of cartilage or bone development at any time.

RG implants. At day 6, matrix particles in RG implants were clearly visible along with invading mesenchymal cells. Occasional chondroblasts were seen around matrix particles. At day 9, areas of cartilage were forming between as well as away from matrix



particles. By day 12 (Fig 4B), the implant was composed of cartilage, mineralized cartilage, and cancellous bone covered with osteoblasts and perforated by vascular channels among a diminished number of matrix particles. Osteoblasts and osteoclasts with positive staining for alkaline phosphatase and TRAP, respectively, were also seen. From days 15 to 42, the RG implants contained remodeling, well-vascularized cancellous bone with a rich hematopoietic marrow analogous to that developed in GE implants (Figs 4D, 7).

DBP implants. At day 6, examination of DBP implants revealed matrix particles surrounded by invading

mesenchymal cells. No evidence of chondrogenesis was apparent. At day 9, a few areas of chondroblasts secreting metachromatic matrix were evident between matrix particles. By day 12 (Fig 6A), DBP implants contained areas of mineralizing cartilage and sparse areas of new bone. Alkaline phosphatase-positive and TRAP-positive cells were present between matrix particles. At days 15 to 21, mineralized cartilage and remodeling bone were present. At day 21, in sites removed from true endochondral ossification of new extracellular matrix, implanted DBP matrix particles were observed to be undergoing remineralization (Fig

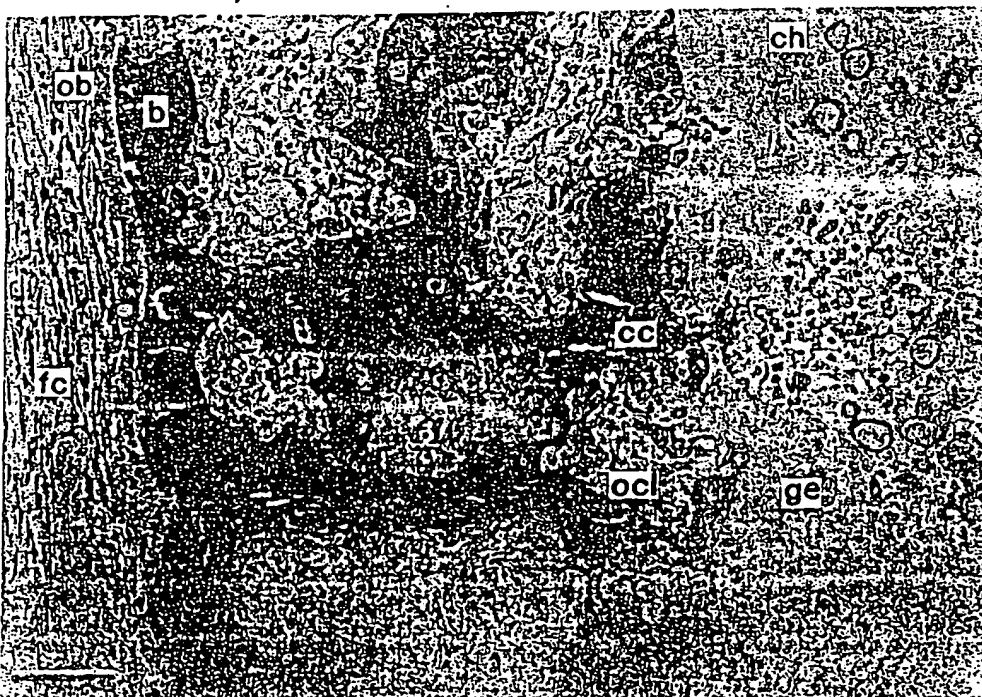


FIGURE 5. Endochondral ossification in a GE20 implant at day 12 (Von Kossa/toluidine blue stain, original magnification $\times 190$, bar = 100 μm). This is a higher power view of Fig 4A. From left to right: fibrous capsule (fc) with small blood vessels (green); osteoblasts (ob) on bone (b); calcified cartilage (cc) undergoing remodeling by osteoclastlike multinucleated giant cells (ocl); chondrocytes (ch) surrounded by metachromatic matrix (red); and flocculated protein (ge) remaining from original implant.

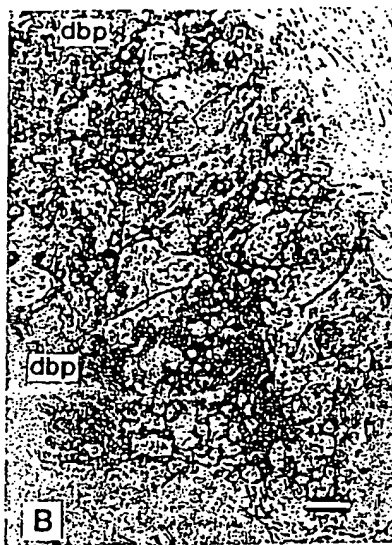
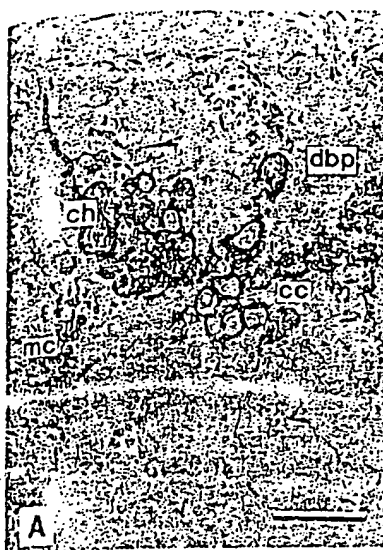


FIGURE 6. *A*, Early stages of endochondral ossification in a DBP implant at day 12 (Von Kossa/toluidine blue stain, original magnification $\times 190$, bar = $100 \mu\text{m}$). Invading mesenchymal cells (mc) and differentiated chondrocytes (ch) producing metachromatic matrix (red) are located between the implanted DBP matrix particles (dbp). Initial cartilage calcification (cc) shows grains of mineral (black) also depositing within the DBP matrix. *B*, Extensive remineralization of DBP particles at day 21 (Von Kossa/toluidine blue stain, original magnification $\times 85$, bar = $100 \mu\text{m}$). Mineral grains (black) extend into DBP particles (dbp), well beyond the extracellular matrix synthesized by the newly differentiated chondrocytes.

FIGURE 7. *A*, Vascularization of new bone in the GE20 implant at day 21 (Von Kossa/toluidine blue stain, original magnification $\times 570$, bar = $50 \mu\text{m}$). Small blood vessels (bv) containing erythrocytes (green) lie close to the surfaces of trabecular bone (b), providing nutrients for the abundant osteoblasts (ob) and trapped osteocytes (oc). *B*, Hematopoietic marrow in the GE20 implant at day 21 (Von Kossa/toluidine blue stain; original magnification $\times 285$, bar = $50 \mu\text{m}$). Osteoblasts (ob) line trabecular bone (b) surfaces; densely packed myeloid cells (my) lie between venous sinusoids (vs) that are filled with erythrocytes (green).

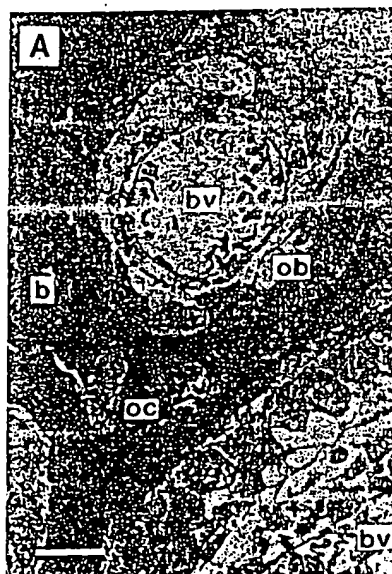


FIGURE 8. *A*, Osteoclastic remodeling in a GE20 implant on day 21 (Von Kossa/toluidine blue stain, original magnification $\times 142$, bar = $100 \mu\text{m}$). Numerous osteoclastlike multinucleated giant cells (ocl) are associated with the remodeling trabecular bone (b) within the implant (Fig 9). *B*, Osteoclasts stained for tartrate-resistant acid phosphatase (TRAP) in a GE20 implant on day 21 (TRAP stain [naphthol AS-MX phosphate/Fast Red TR] counterstained with toluidine blue, original magnification $\times 285$, bar = $50 \mu\text{m}$). Osteoclastlike multinucleated giant cells (ocl) are associated with bone surfaces (b) and stain strongly for TRAP activity (red); osteoblasts (ob) are negative for TRAP.

6B). At days 21 to 42, the DBP implants contained remodeling bone and bone marrow. Eventually the DBP implants are fully remodeled, containing few traces of the implanted particles, but in our experience this has taken 21 to 35 days. In contrast, GE and RG implants are devoid of any traces of implanted particles or protein precipitate by 12 to 18 days and heavily remodeled.

GR implants. At all times, GR implants contained 74 to 250 μm of nonresorbing matrix particles and became surrounded by a thickened connective tissue capsule. No chondrocytes were observed, and there was a total absence of cartilage and bone. Mesenchymal cells did invade between GR particles, and the activity of cathepsin B in GR implants peaked at days 4 to 6 identically to GE10, RG10, and DBP, indicating similar cellular infiltration (data not shown). There was no evidence of the remineralization of matrix particles. In sections from days 12 to 42, no cells stained positively for alkaline phosphatase or TRAP.

HISTOMORPHOMETRY

Histomorphometry was employed on specimens of GE10, RG10, and DBP in an attempt to quantify the qualitative histologic changes reported above. Sections stained with toluidine blue were examined for the presence of metachromatic cartilage and sections stained with von Kossa and toluidine blue were examined for the presence of mineralized bone. Sections stained for TRAP and counterstained with toluidine blue were examined for osteoclasts. Osteoclasts were counted as multinucleated giant cells staining positively for TRAP located on or away from bone surfaces.

GE implants. Cartilage was detected in GE10 sections on days 6 through 12, peaking at 60% to 70% of the total area at day 9; an amount significantly greater than was ever seen in RG10 (40%) or DBP ($\leq 10\%$). Bone was quantifiable from days 12 to 42, occupying about 47% of field area in GE10 by day 42. Osteoclasts were measurable from days 12 to 42, reaching maximal levels on day 15, when a single implant was calculated to contain about 40,000 osteoclasts. This far exceeded the osteoclast density in any other implant type at any time point (Fig 9).

RG implants. Cartilage was quantifiable from days 9 to 15 in lesser amounts than in GE10, but greater than in DBP. Bone was measured on days 12 to 42, with comparable amounts present in RG10 ($32 \pm 6\%$ of area) and GE10 ($47 \pm 10\%$) at day 42. Osteoclasts were quantifiable in amounts consistently less than for GE10 (Fig 9).

DBP implants. Cartilage was relatively scarce in DBP implants at each time point ($\leq 10\%$ of area). Similarly, bone was not quantifiable until day 21, when the approximate 20% bone area did not differ from the

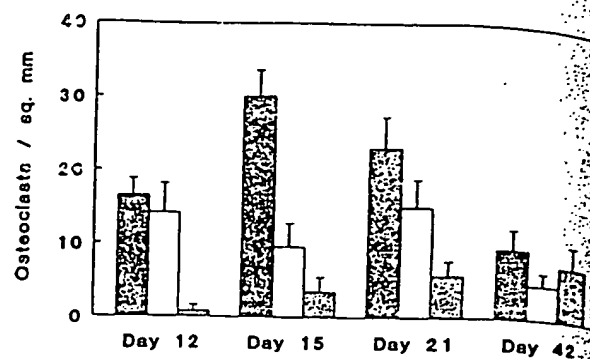


FIGURE 9. Histomorphometric quantitation of osteoclasts in implants at various developmental stages. Representative serial sections from mid-sagittal regions of duplicate implants were examined $\times 200$. Multinucleated giant cells showing a positive TRAP reaction were scored as osteoclasts. Implant groups: GE10 (black bars), RG10 (open bars), DBP (shaded bars); data are means \pm SD. No osteoclastlike cells were ever observed in GR implants. Significantly greater numbers of osteoclasts occurred in GE10 and RG10 compared with DBP at days 12 and 15 ($P \leq .05$). GE10 implants contained 3.1-fold more osteoclasts than RG10 at day 15 ($P \leq .001$). Based on the implant volume and section thickness, a single GE10 implant contained about 40,000 osteoclasts at day 15.

14% to 22% range for GE10 and RG10. At day 42, DBP contained $23 \pm 3\%$ bone area. Osteoclasts were scarce until day 21 when there were four times fewer in DBP fields than in GE10 fields (Fig 9).

MANDIBULAR DEFECTS

Osseous filling of critical size 4-mm bicortical defects in the rat mandibular ramus at days 14 and 21 was achieved equally well by 10 mg of GE or 25 mg of DBP; unimplanted defects remained grossly unfilled at day 21. Histologic examination confirmed the endochondral nature of the filling process, distinguishing it from matrix-mediated osteoconduction. The degree of vascularization of the GE implants was visibly increased compared with DBP at day 21.

Discussion

Subcutaneous implants of GE and RG formulation, as well as DBP, have been clearly demonstrated to induce endochondral bone formation in rats. Most significant is the ability of ethanol-precipitated GE to generate an osteoinductive response, as it plainly demonstrates endochondral bone formation elicited by osteoinductive proteins implanted in the absence of extracellular bone matrix particles. In the experiments reported here, the various stages of endochondral bone formation were readily apparent when examining the response to implants of GE.

Generally, we found that the speed and magnitude of the cellular and biochemical responses increased with increasing dosages of the active GE material. Thus,

12 days it was possible to achieve large increases in the magnitude of osteoinductive parameters (alkaline phosphatase, sixfold; calcium, fivefold) by using GE20 compared with conventional DBP (Fig 3, Table 2). The RG series also showed strong increases over DBP, particularly at the highest 20-mg dose (Figs 2 and 3, Table 2). Chondrogenesis, remodeling, neovascularization, and marrow formation were also enhanced by 10- to 20-mg doses of GE or RG, and the physically largest implants were found with RG20 (Figs 1, 2A). Histomorphometry showed early increases in osteoclast numbers in RG10 and GE10, with GE10 peaking at day 15 with a ninefold greater density than in DBP, and maintaining a fourfold increase at day 21 (Fig 9).

As evidenced by alkaline phosphatase activity, calcium content, and histomorphometry, endochondral bone formation in response to DBP was clearly delayed and diminished when compared with GE and RG implant groups. The observed remineralization of DBP matrix particles (Fig 6B) accounted for much of the total von Kossa-stained mineral phosphate and calls for reassessment of the true amount of bone reflected by the calcium in DBP at day 21 (Fig 3B). If much of the DBP mineral content is actually from remineralization, then the relative performance of GE and RG implants is further enhanced. Nimni and colleagues²⁸ also observed dystrophic calcification of rat DBP implants, hypothesizing that "highly cross-linked collagen may serve as substrate for the deposition of mineral." It should be emphasized that the GE and RG were prepared from the same lot of DBP that yielded the DBP implants. Thus, the DBP itself did contain osteoinductive activity.

GE is a complex mixture of bone macromolecules, containing denatured collagen, matrix Gla protein, GAGs and proteoglycans, polypeptide growth factors including TGF- β 1 and TGF- β 2, and osteoinductive factors OP-1, BMP-2, osteogenin (BMP-3), and other materials.^{4,6-13,29} Thus, it is difficult to ascribe biological effects to a single agent. The extent to which the greatly enhanced chondrogenic response to GE is caused by TGF- β versus OP-1 and BMPs is unknown. Synergistic or antagonistic effects could also pertain to angiogenesis, osteogenesis, remodeling, and hematopoiesis in implants. Because ethanol-precipitated GE is strongly osteoinductive, it will be interesting to discover whether this activity is solely due to the coprecipitation of OP-1/BMPs with collagen/gelatin or is enhanced by the presence of other factors.

Implants of ethanol-precipitated GE may ultimately prove useful as a source of bone cells for study in culture. Particular problems in the study of osteoclasts and osteoclast precursors have been their relative scarcity, fragility, and inability to be isolated as pure cell populations in culture. We estimate the number of active, multinucleated TRAP-positive osteoclasts in a

single day 15 GE10 implant to be about 40,000. Compared with nonvital bone powder implants, the osteoclasts in GE implants were engaged in the resorption of bone in the presence of viable osteoblasts, thus their study *in vitro* may be informative.

Dose dependence of osteoinduction is clearly observed in the RG series (Fig 3), occurring over the studied range of 2- to 20-mg active GE, which was coprecipitated with inert GR to make the RG implants. This contrasts with the relative lack of dose dependence for GE implanted alone (Fig 3). Because of normalization of the alkaline phosphatase and calcium to protein or dry weight, these parameters measure bone quality, not quantity. The GE results suggest that a small dose produces the same intrinsic osteoinductive influence in a small volume as a large dose would in a larger volume; ie, the bone quality of the induced tissue is independent of dose. In contrast, RG-induced bone quality increases sharply with dose (Fig 3). From this we infer that the matrix particles in RG implants may actually present a barrier to the early events in the osteoinductive cascade, and that this can be overcome by filling the interstitial spaces with increasing amounts of precipitated GE material.

Solubilization kinetics of osteoinductive proteins and other physicochemical processes affecting the presentation of these factors to cells are in need of critical analysis. Clearly the form in which GE is delivered is of great importance, producing an osteoinductive biologic response in the order ethanol-precipitated GE > ethanol-precipitated RG > DBP > water-dialyzed GED20. Secondly, the concentration of the factor must be important. Based on the yield of GE from DBP (6 mg/100 mg), a 20-mg GE20 implant contains as much osteoinductive protein as is distributed throughout the particles of 13 separate 25-mg DBP implants. Thus the active agent is delivered in a much more concentrated available form, partially explaining the acceleration and amplification observed in this study. In the future, supplementation of GE with recombinant OP-1 or BMP-2 prior to ethanol precipitation might generate even greater responses.

Several prior reports mention osteoinduction with GE-type materials. Sampath and Reddi,⁴ who originated the ethanol reconstitution procedure, found that lyophilized GE was not osteoinductive, but the exact amounts implanted were not specified. Urist et al³⁰ used BMP enriched fractions in gelatin capsules or filter chambers and reported some dependence on dose. Bolander and Balian¹⁷ augmented rabbit DBP by dialysis with GE from an equivalent amount of bone, testing its efficacy in a rabbit segmental ulnar defect model. At 12 weeks, the augmented implants produced greater mechanical strength than nonaugmented DBP. Thus, by essentially doubling the effective level of osteoinductive protein in the augmented implant, greater

bony healing was achieved. Interestingly, the water dialysis method was effective,¹⁷ whereas our studies with GE20 versus GED20 showed that dialyzed GE is inactive compared with ethanol-precipitated material (Table 2). Muthukumaran et al³¹ implanted "osteogenin enriched fraction" (analogous to our GE) for a single 11-day study in rats. Despite the fact that ethanol precipitation was used, no GE implants smaller than 25 mg were recovered, whereas we recovered 5 and 10 mg implants (Fig 1) in high yield. The 25-mg implant was reported to be osteoinductive, and by coprecipitating with insoluble collagenous bone matrix (ICBM) (analogous to our GR), Muthukumaran et al³¹ were able to see osteoinductive activity in 1 mg of osteogenin-enriched fraction.

Reddi and coworkers have stated that matrix particles of specific size are necessary to allow for mesenchymal cell anchorage, proliferation, and differentiation. They have further suggested that smaller particles are ineffective carriers because they do not have adequate space between them to allow mesenchymal cell invasion and because they allow rapid diffusion of osteoinductive protein(s) away from the site of implantation.^{3-5,20} However, it is evident from the results reported here that matrix particles per se are not necessary as carriers of osteoinductive proteins or as a substrate for mesenchymal cell proliferation. These results are corroborated by the more recent finding that osteogenin implanted without matrix particles into rat craniotomy sites induced bone formation.³²

The use of ethanol-precipitated GE as an osteoinductive agent should provide a direct approach for analyzing the individual effects on developing bone of osteogenic proteins (OP-1, BMPs), endothelial cell growth factors (acidic and basic fibroblast growth factors, aFGF, bFGF), platelet-derived growth factor, and other growth and differentiation factors of relevance to bone.¹³ The rapid attainment by GE implants of a highly vascularized, marrow-filled ossicle (Fig 1) may be of great value in surgical procedures where osteoradionecrosis or other pathologic processes have compromised the recipient site. In principle, induced masses of heterotopic bone also could contribute significantly to hematopoiesis in the host. In this study, however, no gross elevation of white blood cell count or hematocrit was observed in animals bearing two implants of any type.

The formation of bone in response to implanted GE holds promise for the use of osteoinductive protein extracts derived from xenogeneic bone in reconstructive surgery. Advantages may include 1) the avoidance of lengthy and potentially hazardous grinding and sieving of dry bone to a specific particle size, 2) reduction of antigenic, viral, and bacterial components in the implant by eliminating the particulate material, 3) sterilization possibilities for the soluble GE material through ultrafiltration, ultraviolet irradiation, ethanol

treatment, and 4) ease of storage of active protein at -80°C. Xenogeneic osteoinductive proteins could be extracted and processed, and then combined by ethanol precipitation with resorbable or nonresorbable carrier particles for implantation.^{16,32-34}

Conclusions

Osteoinductive implant formulations based on ethanol precipitation of the 4M guanidine-HCl-extractable proteins (GE) of HCl-DBP have been shown to elicit an osteoinductive response even in the absence of implanted bone matrix particles. The response is highly reproducible and follows an endochondral sequence that is accelerated and amplified relative to conventional DBP implants. Ethanol precipitation of GE causes osteoinductive proteins to aggregate in a form that allows them to remain concentrated in the implant site for at least several days, sufficient time for recruitment and transformation of recruited mesenchymal cells. This can also be achieved by the ethanol-mediated adsorption of GE onto the surface of inert GR bone matrix particles. Our findings suggest that the inclusion of bone matrix particles in subcutaneous implants may actually delay and attenuate the initial phases of the osteoinductive response, although it can produce a physically larger mass of heterotopic or orthotopic bone. Finally, ethanol-precipitated GE was fully as effective as DBP in promoting osseous filling of mandibular defects in rats.

Acknowledgment

The technical assistance of G. Hintsch, E. A. Mullen, and S. Wilcox is gratefully acknowledged. Dr J. Glowacki generously provided access to the ZIDAS image analyzer for histomorphometry.

References

1. Urist MR: Bone: Formation by autoinduction. *Science* 150:893-1965
2. Reddi AH, Huggins CB: Biochemical sequences in the transformation of normal fibroblasts in adolescent rats. *Proc Natl Acad Sci USA* 69:1601, 1972
3. Reddi AH: Cell biology and biochemistry of endochondral bone development. *Collagen Rel Res* 1:209, 1981
4. Sampath TK, Reddi AH: Dissociative extraction and reconstitution of extracellular matrix components involved in local bone differentiation. *J Cell Biol* 78:7599, 1981
5. Sampath TK, Reddi AH: Importance of geometry of the extracellular matrix in endochondral bone differentiation. *J Cell Biol* 98:2192, 1984
6. Sampath TK, Muthukumaran N, Reddi AH: Isolation of osteogenin, an extracellular matrix-associated, bone-inductive protein, by heparin affinity chromatography. *Proc Natl Acad Sci USA* 84:7109, 1987
7. Wozney JM, Rosen V, Celeste AJ, et al: Novel regulators of bone formation: Molecular clones and activities. *Science* 242:152-159, 1988
8. Wang EA, Rosen V, Cordes P, et al: Purification and characterization of other distinct bone-inducing factors. *Proc Natl Acad Sci USA* 85:9484, 1988
9. Layton FF, Cunningham NC, Ma S, Muthukumaran N: Purification and partial amino acid sequence of osteogenin.

a protein initiating bone differentiation. *J Biol Chem* 264: 13377, 1989

10. Sampaith TK, Coughlin JE, Whetstone RM, et al: Bovine osteogenic protein is composed of dimers of OP-1 and BMP-2A, two members of the transforming growth factor-beta superfamily. *J Biol Chem* 265:13198, 1990
11. Ozkaynak E, Rueger DC, Drier EA, et al: OP-1 cDNA encodes an osteogenic protein in the TGF- β family. *EMBO J* 9:2085, 1990
12. Reddi AH, Muthukumaran N, Ma S, et al: Initiation of bone development by osteogenin and promotion by growth factors. *Connect Tissue Res* 20:303, 1989
13. Hauschka PV: Growth factor effects in bone, in Hall BK (ed). *Bone: A Treatise, The Osteoblast and the Osteocyte*, vol 1. Caldwell, NJ, Telford Press, 1990, pp 103-70
14. Glowacki J, Altobelli D, Mulliken JB: Fate of mineralized and demineralized osseous implants in cranial defects. *Calcif Tissue Int* 33:71, 1981
15. Kawamura M, Urist MR: Induction of callus formation by implants of bone morphogenetic protein and associated bone matrix noncollagenous proteins. *Clin Orthop* 236:240, 1988
16. Werther JR, Matukas VJ, Miller EJ: A review of matrix-induced osteogenesis with special reference to its potential use in cranio-facial surgery. *Int J Oral Maxillofac Surg* 17:395, 1988
17. Bolander ME, Balian G: The use of demineralized bone matrix in the repair of segmental defects. *J Bone Joint Surg* 68A: 1264, 1986
18. Mark DE, Hollinger JO, Hastings C Jr, et al: Repair of calvarial nonunions by osteogenin, a bone inductive protein. *Plast Reconstr Surg* 86:623, 1990
19. Hollinger JO, Mark DE, Bach DE, et al: Calvarial bone regeneration using osteogenin. *J Oral Maxillofac Surg* 47:1182, 1988
20. Muthukumaran N, Reddi AH: Bone matrix-induced local bone induction. *Clin Orthoped* 200:159, 1985
21. Werther JR, Spampata R, Hauschka PV: Enhanced osteoinduction in a rat bone implant model. *J Dent Res* 66:220, 1987 (abstr)
22. Spampata R, Werther JR, Hauschka PV: Accelerated osteoinduction in a rat bone implant model. *J Bone Min Res* 2:410A, 1987 (suppl 1)
23. Gundberg CM, Hauschka PV, Lian JB, et al: Osteocalcin: Isolation, characterization, and detection. *Meth Enzymol* 107: 516, 1984
24. Kaban LB, Glowacki J: Induced osteogenesis in the repair of experimental mandibular defects in rats. *J Dent Res* 60:1356, 1981
25. Troyer H: Bone alkaline phosphatase kinetics studied by a new method. *Histochemistry* 50:251, 1977
26. Bradford MM: A rapid and sensitive method for the quantification of microgram quantities of protein utilizing the principle of protein-dye binding. *Anal Biochem* 72:248, 1976
27. Rusnock JT, Werther JR, Hauschka PV: Angiogenesis in osteoinductive implants: Quantitation by spectrophotometric assay in a rat model system. *Clin Orthop* (submitted)
28. Nimni ME, Bernick S, Cheung DT, et al: Biochemical differences between dystrophic calcification of cross-linked collagen implants and mineralization during bone induction. *Calcif Tissue Int* 42:313, 1988
29. Hauschka PV, Mavrakos AE, Doleman S, et al: Growth factors in bone matrix: Isolation of multiple types by affinity chromatography on heparin-Sepharose. *J Biol Chem* 261:12665, 1986
30. Urist MR, DeLange RJ, Finerman GAM: Bone cell differentiation and growth factors. *Science* 220:680-6, 1983
31. Muthukumaran N, Ma S, Reddi AH: Dose-dependence of and threshold for optimal bone induction by collagenous bone matrix and osteogenin-enriched fraction. *Collagen Rel Res* 8: 433, 1988
32. Bach DE, Hollinger JO, Mueller J, et al: Comparison of HTR, interpore, and bone inductive agents. *J Oral Maxillofac Surg* 46:M4, 1988
33. Mark DE, Hollinger JO, Quigley N, et al: Bone inductive macroparticles for osseous regeneration. *J Oral Maxillofac Surg* 46:M4, 1988
34. Schnitz JP, Hollinger JO: A preliminary study of the osteogenic potential of a biodegradable alloplastic osteoinductive alloimplant. *Clin Orthop* 237:245, 1988

J Oral Maxillofac Surg
50:151-152, 1992

Discussion

Accelerated Endochondral Osteoinduction in the Absence of Bone Matrix Particles in a Rat Model System

Mark E. Bolander, MD
Mayo Clinic, Rochester, MN

Much recent investigation has focused on characterizing proteins responsible for bone induction in nonosseous tissues. Throughout the course of this work, many (if not all) investigators have observed that successful bone formation depends on the association of specific bone-inducing proteins with a carrier matrix. The application of molecular techniques to the question of bone induction resulted in the isolation and characterization of several proteins, including bone morphogenic proteins (BMPs), osteogenin, and osteogenic protein-1 (OP-1). Cloning and sequencing the genes for these proteins showed that these proteins have significant sequence simi-

larities, and indeed, all are members of a larger group of regulatory proteins, the transforming growth factor β superfamily. Despite the rapid increase in our understanding of these proteins, little is known about the matrix that appears to be required for bone induction.

This study reports the formation of endochondral bone after subcutaneous implantation of proteins derived by ethanol precipitation of a guanidine extract from long bones. Presumably, this precipitate includes not only bone-inducing proteins, but also matrix gla protein, osteonectin, osteocalcin, proteoglycans, collagen type I, and other proteins. This interesting report is the first study showing that although bone formation probably depends on interactions with other proteins, it does not critically depend on the presence of bone matrix particles. This observation has significance for our understanding of the mechanisms of bone induction, and has practical implications for studies attempting to use osteoinductive proteins in surgical situations to augment bone formation.

As the authors indicate in their discussion, it is important to determine the differences between ethanol-precipitated

guanidine extract and dialyzed, lyophilized guanidine extract. These differences could be in the form of the proteins, or alternatively, there could be differences in the composition of the implanted material. Knowing that the guanidine extract is rich in several growth factors, it would be important to determine which components of the guanidine extract are included in the ethanol-precipitated material and how these proteins interact with each other. The authors suggest that the matrix particles may be a barrier to the process of cell differentiation. Alternatively, there may be specific interactions with soluble proteins that influence the attachment of

cells and the availability of cells to interact with protein signals.

Although there will be few limits on the availability or purity of recombinant polypeptides, supplies of natural products such as demineralized bone powder or guanidine extracts of acceptable purity for clinical use will be limited and expensive. The model developed by these authors will facilitate identification of matrix proteins important in the specific interactions necessary for osteoinduction. Understanding these interactions is the key to developing clinical applications for bone-inducing proteins.

**This Page is Inserted by IFW Indexing and Scanning
Operations and is not part of the Official Record**

BEST AVAILABLE IMAGES

Defective images within this document are accurate representations of the original documents submitted by the applicant.

Defects in the images include but are not limited to the items checked:

BLACK BORDERS

IMAGE CUT OFF AT TOP, BOTTOM OR SIDES

FADED TEXT OR DRAWING

BLURRED OR ILLEGIBLE TEXT OR DRAWING

SKEWED/SLANTED IMAGES

COLOR OR BLACK AND WHITE PHOTOGRAPHS

GRAY SCALE DOCUMENTS

LINES OR MARKS ON ORIGINAL DOCUMENT

REFERENCE(S) OR EXHIBIT(S) SUBMITTED ARE POOR QUALITY

OTHER: _____

IMAGES ARE BEST AVAILABLE COPY.

As rescanning these documents will not correct the image problems checked, please do not report these problems to the IFW Image Problem Mailbox.